Spectral Profiling of Autofluorescence Associated with Lipofuscin, Bruch's Membrane, and Sub-RPE Deposits in Normal and AMD Eyes

Alan D. Marmorstein, Lihua Y. Marmorstein, Hirokazu Sakaguchi, and Joe G. Hollyfield

Purpose. To compare the autofluorescence spectra of retinal pigment epithelium (RPE)-associated lipofuscin, Bruch's membrane, and sub-RPE deposits (drusen and basal laminar–linear deposits) in eyes of donors with age-related macular degeneration (AMD) against eyes of age-matched control donors.

Methods. Cryosections were cut from the maculae of unfixed human donor eyes with AMD or from age-matched control eyes. Tissues were excited at wavelengths of 364, 488, 568, and 633 nm. Emission spectra were collected with a confocal microscope equipped with a spectrophotometric detector at 10-nm wavelength intervals between 400 and 800 nm.

Results. RPE lipofuscin had strong autofluorescent emissions that were excited at all wavelengths. Bruch's membrane exhibited strong autofluorescence with an emission peak of 485 ± 5 nm when excited with 364-nm light. At 488-, 568-, and 633-nm excitations, Bruch's membrane and sub-RPE deposits in normal eyes exhibited minimal autofluorescence. In AMD eyes, however, both the 364- and 488-nm excitation wavelengths stimulated substantial blue-green emissions from sub-RPE deposits and Bruch's membrane, with average pixel intensities substantially exceeding that elicited in the yellow-orange range by RPE lipofuscin.

Conclusions. These data suggest that an increase in blue-green autofluorescence of Bruch's membrane relative to the yellow-orange autofluorescence of RPE-associated lipofuscin is associated with AMD. Knowledge of these spectra will be useful in evaluating animal models of macular degenerative disease and in diagnosis of AMD, and will provide a novel signature for further analysis of the molecular entities emitting these fluorescent signatures. (*Invest Ophthalmol Vis Sci.* 2002;43: 2435–2441)

Age-related macular degeneration (AMD) is the leading cause of blindness in the Western world, affecting nearly 30% of those over the age of 75.[1] AMD alters the quality of life of those affected by causing a debilitating loss of central vision. Clinically, the disease is characterized by an increase in macular drusen and mottling of the RPE or areas of geographic atrophy and in some cases by choroidal neovascularization.[2] Histopathologically, AMD is characterized by photoreceptor cell loss, hyperplasia and/or atrophy of RPE cells, abnormal thickening of Bruch's membrane, and a variety of sub-RPE deposits (i.e., soft drusen and basal laminar deposits).[3] In late stages, calcification of Bruch's membrane is also observed.[3] Although a relationship between lipofuscin content of the RPE and AMD has been suggested,[4] no quantitative analysis has fully examined the relationship. Despite the described characteristics, hard drusen and accumulation of lipofuscin can be found in nearly all eyes, increasing with age.[5–7]

Lipofuscin is a ubiquitous material present in granules in the RPE cell with a characteristic UV-excitable fluorescence[8] that is accounted for in part by A2E, the product of hydrolysis of vitamin A aldehyde and phosphatidylethanolamine.[9–11] In Stargardt's disease, a relationship between lipofuscin accumulation and retinal degeneration is strongly supported by studies of the *abcr* knockout mouse.[12] The recent development of the confocal scanning laser ophthalmoscope (cLSO) has greatly facilitated the study of fundus autofluorescence in humans. Studies using the cLSO and other means of measuring fundus autofluorescence have been, for the most part, limited to inherited maculopathies such as Stargardt's disease, in which an enhanced accumulation of lipofuscin is better established,[13–18] or to patients in whom AMD has progressed to geographic atrophy.[19–23] These studies have focused primarily on fluorescent emissions that represent RPE-associated lipofuscin.[24] Although some studies suggest that fundus autofluorescence may be elevated in areas peripheral to regions of geographic atrophy[21,23] or in advance of atrophy,[22] fundus autofluorescence measurements have not gained wide acceptance as a diagnostic tool. Although there is a growing body of evidence linking lipofuscin accumulation with RPE atrophy,[4] the connection between lipofuscin and AMD remains tenuous.

Lipofuscin granules in the RPE are not the only autofluorescent entities in the posterior pole of the eye. Autofluorescence of Bruch's membrane and drusen have also been anecdotally reported,[25–27] although the spectrum has never been characterized. More recently, it has been observed in a systematic study of fundus autofluorescence, that the spectrum in regions with drusen is shifted toward shorter wavelengths.[20,28]

To better understand the individual autofluorescence spectra of sub-RPE deposits, Bruch's membrane, and RPE lipofuscin, we took advantage of recent developments in confocal microscopy that allow the collection of emission spectra from *X–Y* scans of tissue sections. Using a laser scanning confocal microscope with a spectrophotometric detector, we determined that Bruch's membrane and sub-RPE deposits had overlapping spectra that were excited by UV and blue light with fluorescent emissions in the blue-green spectrum. Furthermore, this fluorescence was increased compared with lipofuscin fluorescence in eyes of donors with AMD relative to eyes of age-matched control donors.

From the Department of Ophthalmic Research, Cole Eye Institute, The Cleveland Clinic Foundation, Cleveland, Ohio.

Presented at the annual meeting of the Association for Research in Vision and Ophthalmology, Fort Lauderdale, Florida, May 2001.

Supported by National Institutes of Health Grant R01-EY13160 (ADM), a Kirchgessner Foundation research grant (ADM), the Foundation Fighting Blindness (JGH), and the Cleveland Clinic Foundation.

Submitted for publication June 19, 2001; revised March 1, 2002; accepted March 13, 2002.

Commercial relationships policy: N.

The publication costs of this article were defrayed in part by page charge payment. This article must therefore be marked *"advertisement"* in accordance with 18 U.S.C. §1734 solely to indicate this fact.

Corresponding author: Alan D. Marmorstein, Cole Eye Institute, i-31, The Cleveland Clinic Foundation, 9500 Euclid Avenue, Cleveland, OH 44195; marmora@ccf.org.

METHODS

Tissues

Three eyes of normal human donors of both sexes aged 81, 83, and 87 years and three eyes of AMD donors aged 74, 84, and 92 years were used in this study. AMD donor eyes were obtained through the Eye Donor Program of the Foundation Fighting Blindness (Hunt Valley, MD). The use of human tissue was in accordance with the tenets of the Declaration of Helsinki. Eyes were enucleated between 2 and 6 hours after death and preserved at 4°C for 1 to 14 hours. The eyes with AMD have been characterized by Kamei and Hollyfield,[29] and are the eyes numbered 359, 444, and 447 in Table 2 in the former study. Histopathologic characterization indicated that donor 359 had extensive soft drusen, donor 444 had soft drusen and choroidal neovascularization, and donor 447 had extensive hard and soft drusen. Age-matched control eyes were obtained through the Cleveland Eye Bank (Cleveland, OH), and the National Disease Research Interchange (NDRI, Philadelphia, PA). Immediately after arrival in our laboratory or at NDRI, the eyes were frozen in liquid nitrogen and stored at −80°C until preparation of samples.

Tissue Preparation

Each sample consisted of a 2-mm-wide strip of the retina-RPE-choroid-sclera complex, centered on the fovea. Unfixed samples were embedded in optimal cutting temperature compound (OCT; Miles Diagnostics, Elkhart, IN) and frozen in liquid nitrogen. Cryosections (8 μm thick) were air dried on slides for 30 to 40 minutes, and then OCT was removed by a 5-minute wash in water. Samples were again air dried for 30 minutes and then mounted in fluorescent mounting medium (Fluormount; Electron Microscopy Sciences, Fort Washington, PA).

Confocal Microscopy

Wavelength scans were performed using the 364-, 488-, 568-, and 633-nm laser lines of a laser scanning confocal microscope (TCS-SP; Leica, Deerfield, IL) equipped with a spectrophotometric detector utilizing a Hamamatsu R6357 photodetector (Hamamatsu Corp., Hamamatsu City, Japan). This detector exhibits relatively even radiant sensitivity and quantum efficiency in the 400- to 800-nm range. Data as presented are not corrected for changes in sensitivity of the detector at different wavelengths. The spectrophotometric detector used does not rely on barrier filters, and so filter characteristics did not influence the spectrum. Scans were performed using the substrate (for UV) or SP30/70 splitters (visible light), with an open pinhole, and the detector was set to advance a 10-nm window of detection in 10-nm increments between 400 and 800 nm. Gains were set individually for each field at each excitation wavelength, by using the glow over- under function to optimize collection of data across the full 8-bit scale. This was accomplished in a 10-nm window determined by narrowing the window of detection during continuous scanning to the region of maximum fluorescence. Gains were not altered through the course of the scan. Each scan was performed using frame averaging set at 4. Data were acquired in 8-bit mode starting with the 633-nm laser and progressing to shorter wavelengths in order. Lasers were set in the park position, resulting in delivery of 200 mW for the UV Ar laser (364-nm excitation) and 300 mW for the Ar and Kr lasers (488- and 568-nm excitation) to the back of the aperture lens according to the manufacturer's specifications. The HeNe laser (633-nm excitation) was set to deliver 1 mW to the back of the aperture lens according to the manufacturer's specifications.

Average pixel intensities for Bruch's membrane, sub-RPE deposits, and RPE-lipofuscin were determined on computer (Metamorph software ver. 4.5; Universal Imaging, West Chester, PA, running on a Pentium III-powered computer; Intel Corp., Mountain View, CA). Numerical data were exported to a spreadsheet (Excel 97; Microsoft, Redmond, WA). The significance of differences in spectra obtained between control and AMD-affected eyes was assessed using a two-tailed, two-sample *t*-test, with no variance assumptions run within the software (Excel 97; Microsoft). Bruch's membrane and sub-RPE deposits were selected for analysis based on a differential interference contrast (DIC) image of each field analyzed. Drusen and basal laminar-linear deposit were distinguished on the basis of shape. Hard and soft drusen were defined by their round contours with clearly defined borders. We could not always distinguish between soft and hard drusen by DIC imaging. Basal laminar and basal linear deposits (BLDs) were defined as a thick continuous layer of accumulations beneath the RPE. We could not distinguish basal laminar and basal linear deposits. Drusen and BLDs were not found to have different spectra and therefore were not separated in the final analysis of the data. Therefore, for the purposes of this study we referred to drusen and BLD collectively as sub-RPE deposits. Lipofuscin granules were selected by thresholding the section in each data set with the brightest RPE-lipofuscin to reveal the specific granules. Average pixel intensities for the Bruch's membrane, sub-RPE deposits, and RPE-lipofuscin from the same fields were normalized against the strongest measurement associated with lipofuscin in each section series. To control for photobleaching, a separate set of sections were scanned sequentially as just described, progressing from 633- through 364-nm excitation, and then rescanned. This resulted in a shift of the background relative to the signal in the second scan of approximately 10% of maximum pixel intensity across the image.

RESULTS

To examine the autofluorescent emissions of tissue with respect to its origin, 8-μm sections derived from maculae of unfixed posterior poles were prepared, and three sections from each eye were examined by confocal microscopy using light at 633, 568, 488, and 364 nm for excitation. *XY*-λ data sets, comprising a series of two-dimensional (*XY*) images stacked so that the *Z*-coordinate is λ, were accumulated for emitted light in 10-nm increments from 400 to 800 nm. Each *XY*-λ data set comprises a section series that was analyzed as a whole. The peak emission generated at λ_{ex} by reflection of the excitation stimulus is omitted from all section series presented where λ_{ex} is 488 nm or more.

Representative DIC images are shown in Figure 1 for control (Fig. 1A) and AMD (Fig. 1B) samples. All control samples contained hard drusen similar to the one shown in Figure 1A, and fields were deliberately chosen to include drusen. More variability was present in the AMD samples (Fig. 1B). Not all fields from eyes with AMD contained drusen, although all contained some form of deposit between the RPE and Bruch's membrane. The most common finding was BLD. BLD was absent from all fields in control eyes.

Spectral scans were performed starting with λ_{ex} of 633 nm and moved to progressively shorter wavelengths to minimize any potential for photobleaching. The emission peak (λ_{max}) for Bruch's membrane, sub-RPE deposits, and lipofuscin at each excitation wavelength are reported in Table 1. At λ_{ex} of 633 and 568 nm in both control and AMD samples (Fig. 2), the dominant signal emanated from RPE-associated lipofuscin. Very small differences were noted in the λ_{max} associated with each of the regions examined. These differences were confined to slight blue shifts of sub-RPE deposits and Bruch's membrane relative to lipofuscin. Because the λ_{max} for these structures was within 10 nm, in effect they all had the same spectrum (Fig. 2). An increase in the intensities of both Bruch's membrane and sub-RPE deposits was noted in eyes with AMD, although this difference failed to show significance in a two-sample *t*-test.

At λ_{ex} of 488 nm, a 10- to 15-nm difference was reproducibly obtained between the spectra elicited from Bruch's membrane and the sub-RPE deposits in comparison with lipofuscin

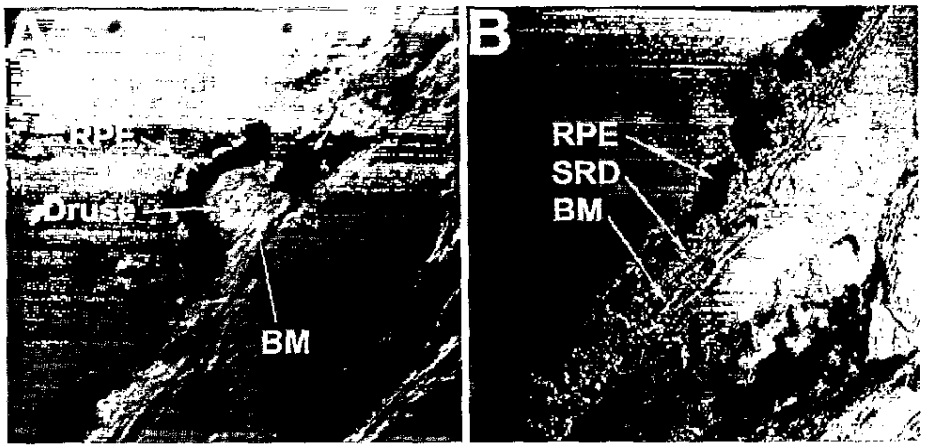

FIGURE 1. Representative DIC images of eyes used in this study. (A) A typical field from a control eye, in this case an 81-year-old female donor. Note the hard druse in the center of the field. This was typical of the drusen that were encountered in control eyes. (B) Eye of a 92-year-old male donor with AMD. Note the extensive basal laminar sub-RPE deposit (SRD) and increased birefringence of Bruch's membrane (BM).

(Fig. 3). The difference in λ_{max} (Table 1) was identical in both control eyes and eyes with AMD.

In Table 2, the percentage of maximum fluorescence intensity is shown for the λ_{max} for sub-RPE deposits, Bruch's membrane, and lipofuscin at each excitation wavelength. Values are normalized to the intensity of lipofuscin at the λ_{max} obtained in Table 1. Therefore, within a sample lipofuscin intensity can vary from 100% if there is variability in λ_{max} between section series or between donor eyes. Normalization of the signals in this way permits comparison of the intensity at the λ_{max} of each spectrum and indicates the strongest signal and reproducibility of that signal intensity for each region and spectrum at a given λ_{ex}. Quantitative comparisons of intensity among spectra derived with different λ_{ex} are not valid because of differences in detector gain settings and laser power. For this reason, all comparisons were made between the spectra elicited from sub-RPE deposits, Bruch's membrane, and lipofuscin with the same λ_{ex}.

At λ_{ex} of 488 nm, lipofuscin was the dominant autofluorescent entity in control eyes (Table 2). A substantial increase in the intensity of the Bruch's membrane fluorescence was detected in the AMD-affected eyes when compared with lipofuscin fluorescence. In control eyes the Bruch's membrane normalized fluorescence at λ_{max} was 53% ± 13% (mean ± SEM), whereas in eyes with AMD the normalized Bruch's membrane's fluorescence was 112% ± 29%. Application of the *t*-test to these measurements resulted in $P = 0.07$. Despite the differences in Bruch's membrane's fluorescence, no difference was detected in the normalized intensity of sub-RPE deposits in control (57 ± 17%) versus AMD-affected eyes (60% ± 5%).

TABLE 1. λ_{max} for Bruch's Membrane, Sub-RPE Deposits, and RPE

λ_{ex} (nm)	Specimen	Bruch's Membrane	Sub-RPE Deposits	RPE
364	Control	485	485	555
	AMD	485	490	540
488	Control	540	545	555
	AMD	540	545	555
568	Control	610	610	615
	AMD	600	605	615
633	Control	645	645	655
	AMD	650	650	655

λ_{max} data are ±5 nm. Data are presented as means derived from three eyes in which at least three fields were examined.

At λ_{ex} of 364 nm, a substantial difference was found between λ_{max} (Table 1, Fig. 4) for Bruch's membrane and sub-RPE deposits compared with lipofuscin. In both control and AMD eyes, Bruch's membrane exhibited a λ_{max} of 485 ± 5 nm, similar to the λ_{max} obtained for sub-RPE deposits. However lipofuscin had a λ_{max} of 555 ± 5 nm in control eyes and 540 ± 5 nm in eyes with AMD. Thus, we could clearly delineate different spectra for Bruch's membrane and sub-RPE deposits with respect to lipofuscin. In AMD-affected eyes, Bruch's membrane was clearly the brightest source of fluorescence (Table 2) excited by 364-nm light. Furthermore, a substantial difference was found in the normalized intensity of Bruch's membrane's fluorescence in AMD-affected versus control eyes. This difference (82% ± 9%) in control eyes versus. 154 ± 10 in eyes with AMD was significant ($P = 0.03$). A small difference was noted for sub-RPE deposits, as well with sub-RPE deposits: 77% ± 4% of the intensity of lipofuscin in control eyes and 96% ± 12% in AMD-affected eyes, although this difference was not significant ($P = 0.37$).

DISCUSSION

Early diagnosis is the key to successful preventative medicine. The apparent changes in fundus autofluorescence in AMD and other retinal degenerative diseases[15–25] suggests that these measurements could serve as an early diagnostic test or prognostic indicator. We examined the autofluorescence spectra of three components of the posterior pole of the eye—Bruch's membrane, sub-RPE deposits, and lipofuscin granules within the RPE—in part, with the goal of characterizing their individual contributions to fundus autofluorescence. We found that Bruch's membrane and sub-RPE deposits can contribute substantially to the autofluorescent spectrum of the fundus when excited with 364- or 488-nm light. We also characterized a novel ~485 ± 5-nm peak of fluorescence excited from Bruch's membrane and sub-RPE deposits with 364-nm light.

The finding that Bruch's membrane and sub-RPE deposits exhibit their own fluorescence is important, in that it must contribute to the image obtained when examining fundus autofluorescence. However, the contribution to the fundus image differs from that which we describe. Although we can make statements about the ratio of emissions generated from one region (i.e. Bruch's membrane) in comparison to another (i.e. lipofuscin), these are separated by virtue of the magnification at which we are working (×400 in all cases), and the use of radial sections of the outer eye wall. In vivo autofluorescence measurements are made in what would be an en face

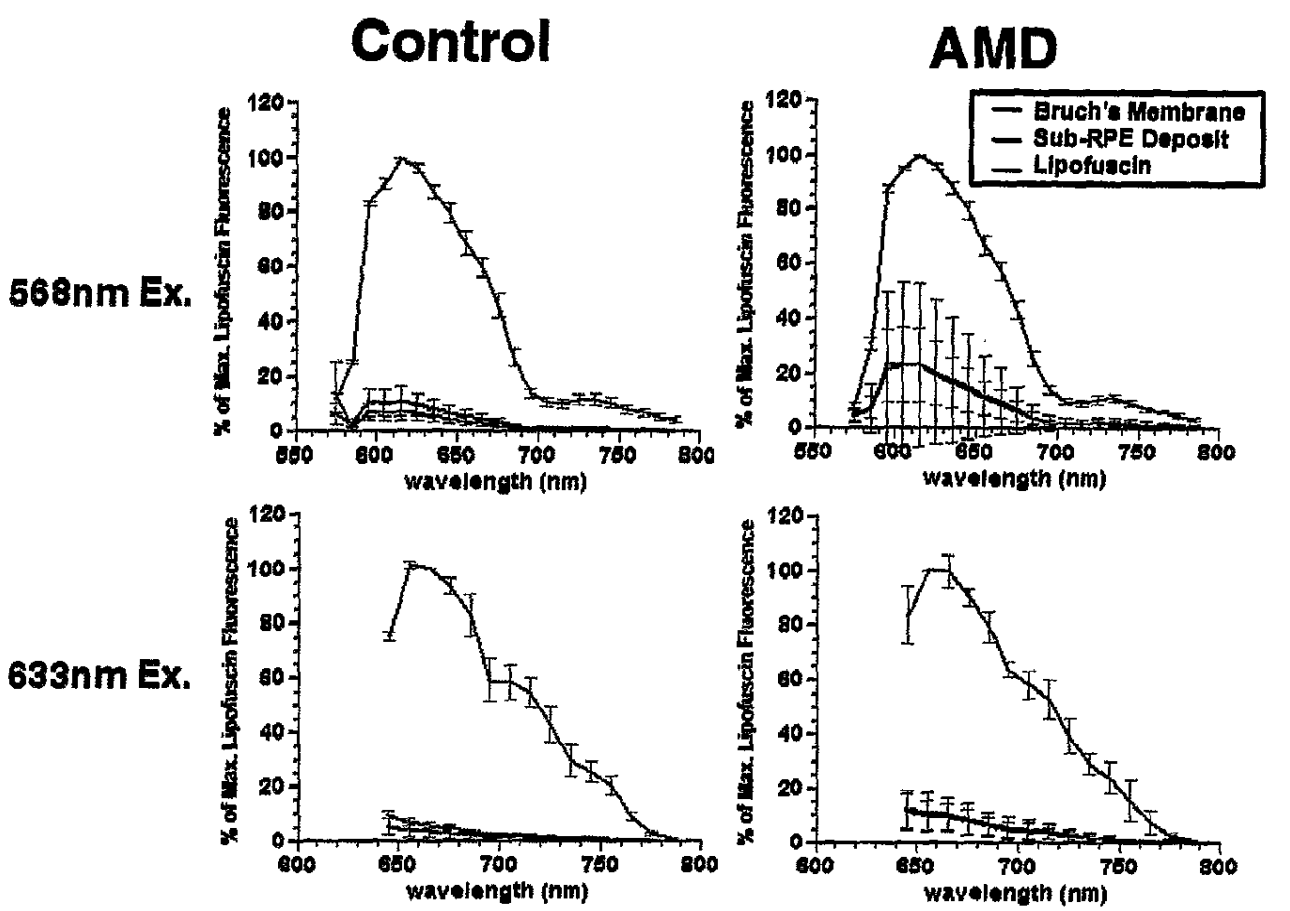

FIGURE 2. Spectral profiles derived using λ_{ex} of 568 and 633 nm. Data are representative spectra from individual donor eyes. Lipofuscin is indicated by *red line*, sub-RPE deposits by *green*, and Bruch's membrane by *blue*. Data are the mean ± SD from the three fields examined in each eye. No significant difference was observed between control and AMD-affected eyes with λ_{ex} of either 568 or 633 nm.

orientation under the microscope and without the vertical resolution necessary to separate Bruch's membrane, sub-RPE-deposits, and lipofuscin. Furthermore, the contribution of a druse may be substantially greater if it is large and viewed en face, as opposed to in the 8-μm-thick sections that we used. Indeed, others[20,28] have shown that in eyes with drusen, there is a measurable blue shift in fundus autofluorescence. Our data confirm these earlier observations and suggest that the shift is in fact due to the novel spectrum of sub-RPE deposits compared with lipofuscin. Unfortunately, because of the limited availability of donor eyes with AMD en face sections were not available for this study.

Also of interest is the finding that the fluorescence intensity of Bruch's membrane exceeds that of lipofuscin in AMD eyes when excited with 364-nm light. This could be due to two possibilities. The first is loss of RPE cells and thinning of the cells resulting in a decrease in lipofuscin granules. This possibility however can be ruled out in the context of this study, as the regions selected for measurement included only those with RPE cells, lipofuscin granules were specifically selected as opposed to whole cells, and the use of radial-sections eliminates thinning of the RPE from consideration. The second possibility is that the blue autofluorescence of Bruch's membrane is in fact increased in AMD-affected eyes relative to control eyes. A qualitative examination of the sections suggests that this is in fact the case. Though it is tempting to speculate on the molecular entities responsible for this fluorescence, a large number of compounds could, alone or in combination, be responsible for this spectrum.

Can this spectrum be used diagnostically? It is tempting to suggest that quantitative measurement of the Bruch's membrane's autofluorescence could serve as a diagnostic tool for AMD, and in fact we describe herein a novel spectrum that differs in intensity in control eyes and eyes with AMD. Unfortunately, this spectrum is excited by UV light that is blocked from entering the eye by the cornea and lens. Furthermore, in our studies the pigment granules of the RPE did not influence the delivery of light to the sample. Changing to an en face orientation would place the RPE pigment granules between Bruch's membrane and the light source, as well as between Bruch's membrane and a detector, potentially quenching the effect that we describe in radial section. However, the increase in fluorescence observed using 488-nm light could be put to use. Barring a damping effect of the pigment granules, the total fluorescence detected when excited by 488-nm light should be increased relative to control eyes. Earlier fundus autofluorescence studies used 510- or 470-nm excitation wavelengths.[23,28]

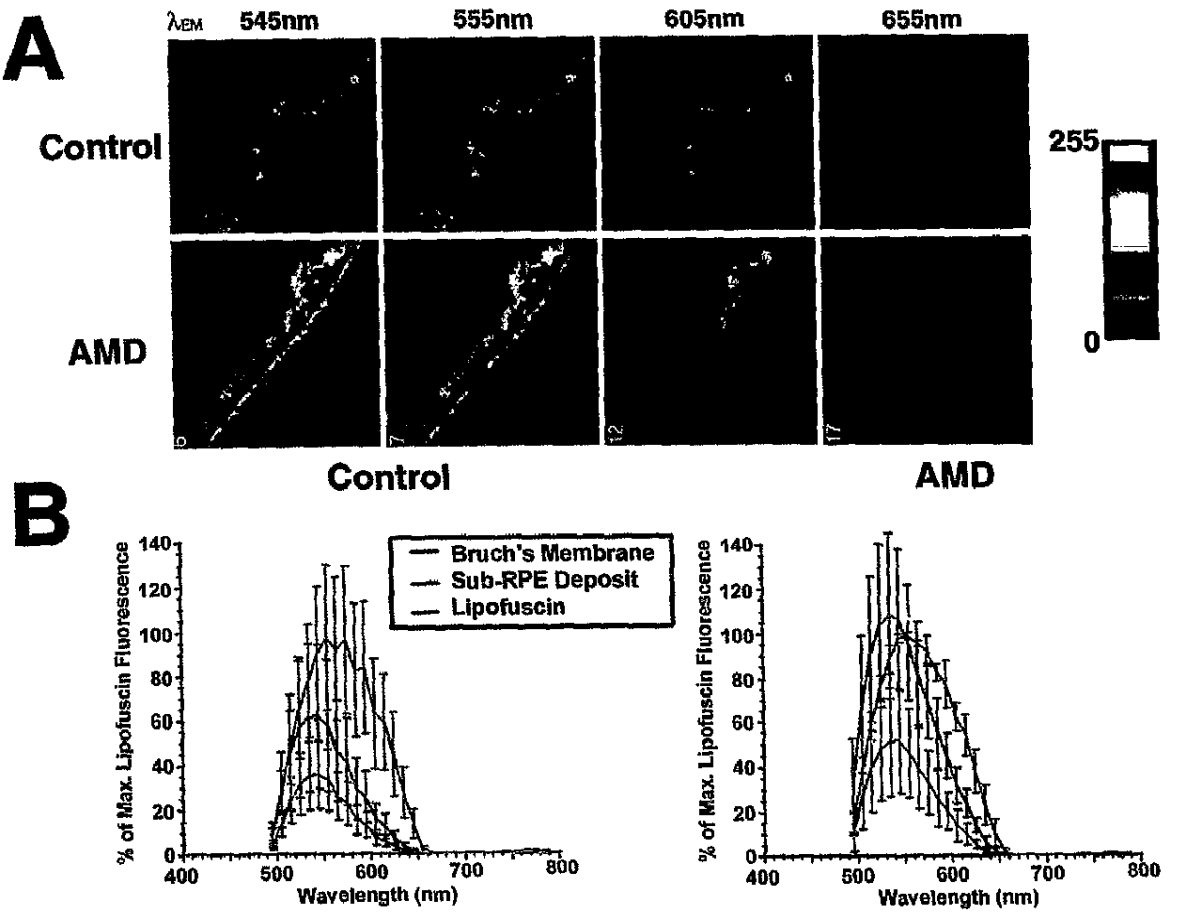

FIGURE 3. Spectrum of Bruch's membrane, sub-RPE deposits, and lipofuscin using λ_{ex} of 488 nm. (A) Pseudocolor representation from control and AMD spectral data sets. Each panel derives from a select 10-nm window centered on the indicated λ. The pseudocolor scale is shown on the *right*. (B) Sample spectra from representative donor eyes. Data are the mean ± SD from the three fields examined in each eye. Note the increase in Bruch's membrane's intensity in the AMD-affected eye relative to lipofuscin.

In those studies, lipofuscin fluorescence was found to be more efficiently excited at 510 nm with a greater contribution derived from sub-RPE deposits when λ_{ex} was 470 nm. One difference from our findings is that others have found that peak lipofuscin fluorescence in vivo exhibits a λ_{max} of 620 nm as opposed to the 555 nm we observed. This could be in part due to the difference in excitation wavelength—510 nm in the former studies as opposed to 488 nm in the present study—and to macular pigment or age-associated yellowing of the lens.

TABLE 2. Percentage Maximum Pixel Intensities of Bruch's Membrane, Sub-RPE Deposits, and Lipofuscin

λ_{ex} (nm)	Specimen	Bruch's Membrane	Sub-RPE Deposits	Lipofuscin
364	Control	82 ± 9	77 ± 4	96 ± 2
	AMD	154 ± 10	96 ± 12	97 ± 1
488	Control	53 ± 13	57 ± 17	97 ± 2
	AMD	112 ± 29	60 ± 5	100 ± 1
568	Control	31 ± 10	21 ± 7	100
	AMD	45 ± 9	33 ± 4	100
633	Control	9 ± 1	11	100
	AMD	15 ± 3	15 ± 4	100

Data are mean ± SEM (n = 3 eyes) and are normalized against the brightest point of lipofuscin fluorescence in each section series. The brightest source of fluorescence was assigned 100%. SEM associated with lipofuscin indicates slight variability in λ_{max} of lipofuscin between eyes.

In healthy eyes, we found that the λ_{max} of lipofuscin in RPE cells was 555 nm when excited with light at 364 nm, similar to the 565 λ_{max} reported by Sparrow et al.[30] for A2E in unfixed RPE cells excited with 380-nm light. We also found that the emission spectrum of lipofuscin shifted gradually toward the red as the excitation wavelength was increased, similar to the data reported by Delori.[24] The shift of λ_{max} to 540 nm that we observed for lipofuscin in AMD-affected eyes may be due to overlap of RPE and sub-RPE deposits in some sections from those eyes, or could represent a real change in the spectral characteristics and thus the composition of lipofuscin in eyes with AMD.

In summary, we examined the autofluorescent spectra of Bruch's membrane, sub-RPE deposits, and lipofuscin in AMD-affected and age-matched control eyes. We found a novel UV-excitable spectrum associated with Bruch's membrane and sub-RPE deposits that appears to be present at higher intensities in AMD-affected eyes than in age-matched control eyes.

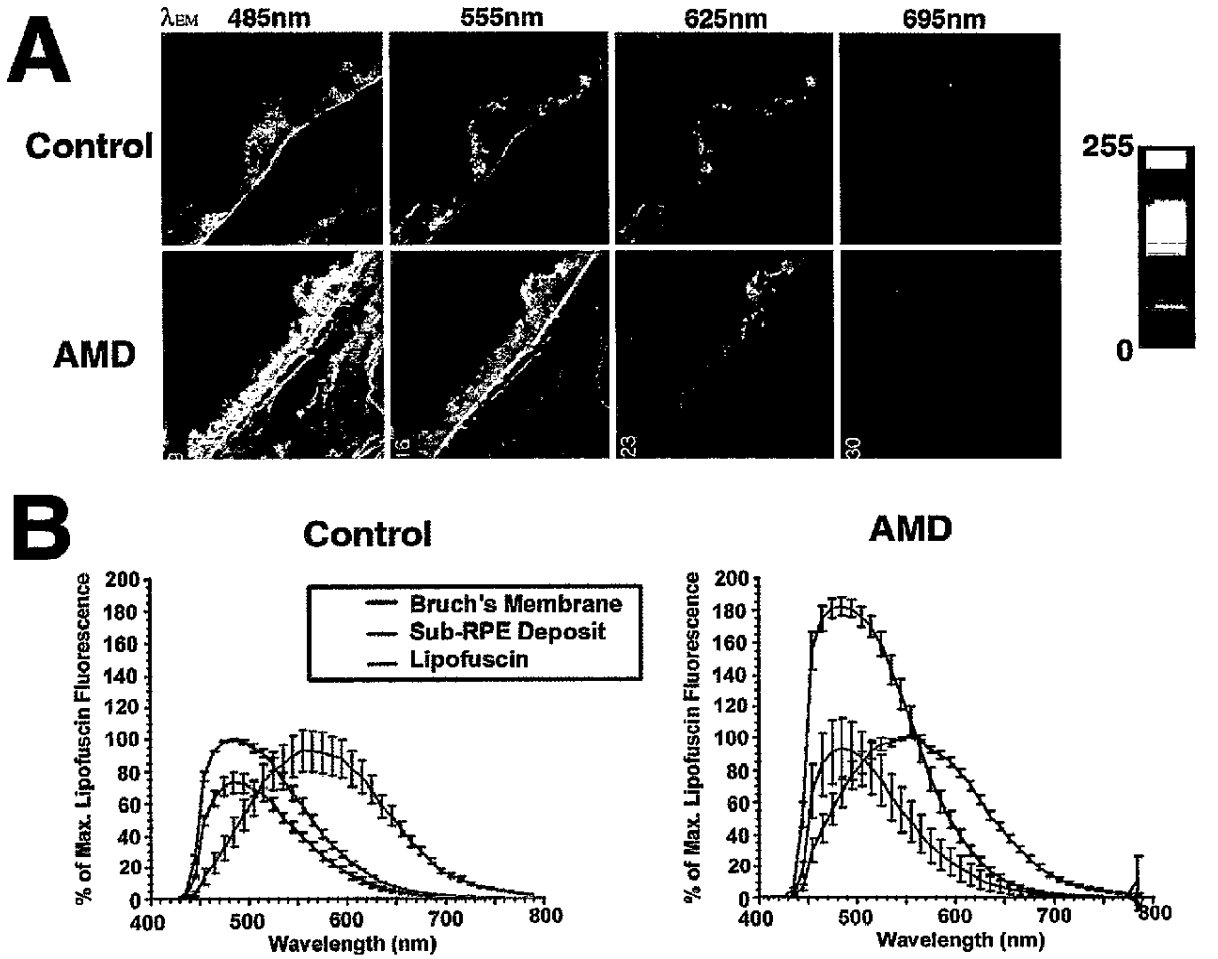

FIGURE 4. Spectrum of Bruch's membrane, sub-RPE deposits, and lipofuscin using λ_{ex} = 364 nm. (A) Pseudocolor representation of select 10-nm windows centered on the indicated λ from control and AMD spectral data sets. The pseudocolor scale is shown on the right. (B) Sample spectra from representative donor eyes. Data are the mean ± SD from the three fields examined in each eye. Note the increase in Bruch's membrane's intensity in the AMD-affected eye relative to lipofuscin.

Acknowledgments

The authors thank Judy Drazba and Amit Vasanji of the Lerner Research Institute imaging core and Vladimir Zhukarev of Leica Imaging Systems for their assistance in acquiring confocal images, and Jason Connor for assistance with statistical analysis of the data.

References

1. Leibowitz HM, Krueger DE, Maunder LR, et al. The Framingham Eye Study monograph: an ophthalmological and epidemiological study of cataract, glaucoma, diabetic retinopathy, macular degeneration, and visual acuity in a general population of 2631 adults, 1973–1975. *Surv Ophthalmol.* 1980;24(suppl):335–610.
2. Gass DJM. Heredodystrophic disorders affecting the pigment epithelium and retina. In: Gass DJM, ed. *Diagnosis and Treatment.* St. Louis: Mosby; 1997:303–313. *Stereoscopic Atlas of Macular Diseases*; vol. 1.
3. Green WR, Enger C. Age-related macular degeneration histopathologic studies: the 1992 Lorenz E. Zimmerman Lecture. *Ophthalmology.* 1993;100:1519–1535.
4. Winkler BS, Boulton ME, Gottsch JD, et al. Oxidative damage and age-related macular degeneration. *Mol Vis.* 1999;5:32.
5. Lewis H, Straatsma BR, Foos RY. Chorioretinal juncture: multiple extramacular drusen. *Ophthalmology.* 1986;93:1098–1112.
6. Feeney-Burns L, Hilderbrand ES, Eldridge S. Aging human RPE: morphometric analysis of macular, equatorial, and peripheral cells. *Invest Ophthalmol Vis Sci.* 1984;25:195–200.
7. Kitagawa K, Nishida S, Ogura Y. In vivo quantitation of autofluorescence in human retinal pigment epithelium. *Ophthalmologica.* 1989;199:116–121.
8. Eldred GE, Miller GV, Stark WS, et al. Lipofuscin: resolution of discrepant fluorescence data. *Science.* 1982;216:757–759.
9. Eldred GE, Lasky MR. Retinal age pigments generated by self-assembling lysosomotropic detergents. *Nature.* 1993;361:724–726.
10. Sakai N, Decatur J, Nakanishi K, Eldred GE. Ocular age pigment A2-E: an unprecedented pyridinium bisretinoid. *J Am Chem Soc.* 1996;118:1559–1560.
11. Liu J, Itagaki Y, Ben-Shabat S, et al. The biosynthesis of A2E, a fluorophore of aging retina, involves the formation of the precursor, A2-PE, in the photoreceptor outer segment membrane. *J Biol Chem.* 2000;275:29354–29360.
12. Weng J, Mata NL, Azarian SM, et al. Insights into the function of Rim protein in photoreceptors and etiology of Stargardt's disease from the phenotype in abcr knockout mice. *Cell.* 1999;98:13–23.

13. Barr DB, Beirouty ZA. Autofluorescence in a patient with adult vitelliform degeneration. *Eur J Ophthalmol.* 1995;5:155–159.
14. Downes SM, Fitzke FW, Holder GE, et al. Clinical features of codon 172 RDS macular dystrophy: similar phenotype in 12 families. *Arch Ophthalmol.* 1999;117:1373–1383.
15. Lois N, Holder GE, Fitzke FW, et al. Intrafamilial variation of phenotype in Stargardt macular dystrophy-Fundus flavimaculatus. *Invest Ophthalmol Vis Sci.* 1999;40:2668–2675.
16. Lois N, Holder GE, Bunce C, et al. Phenotypic subtypes of Stargardt macular dystrophy-fundus flavimaculatus. *Arch Ophthalmol.* 2001; 119:359–369.
17. Miller SA. Fluorescence in Best's vitelliform dystrophy, lipofuscin, and fundus flavimaculatus. *Br J Ophthalmol.* 1978;62:256–260.
18. von Ruckmann A, Fitzke FW, Bird AC. In vivo fundus autofluorescence in macular dystrophies. *Arch Ophthalmol.* 1997;115: 609–615.
19. Armstrong D, Gum G, Webb A. et al. Quantitative autofluorescence in the ovine and canine ocular fundus in ceroid-lipofuscinosis (Batten's disease). *Vet Res Commun.* 1988;12:453–456.
20. Delori FC, Fleckner MR, Goger DG. et al. Autofluorescence distribution associated with drusen in age-related macular degeneration. *Invest Ophthalmol Vis Sci.* 2000;41:496–504.
21. Holz FG, Bellmann C, Margaritidis M, et al. Patterns of increased in vivo fundus autofluorescence in the junctional zone of geographic atrophy of the retinal pigment epithelium associated with age-related macular degeneration. *Graefes Arch Clin Exp Ophthalmol.* 1999;237:145–152.
22. Holz FG, Bellman C, Staudt S, et al. Fundus autofluorescence and development of geographic atrophy in age-related macular degeneration. *Invest Ophthalmol Vis Sci.* 2001;42:1051–1056.
23. Solbach U, Keilhauer C, Knabben H, et al. Imaging of retinal autofluorescence in patients with age-related macular degeneration. *Retina.* 1997;17:385–389.
24. Delori FC, Dorey CK, Staurenghi G, et al. In vivo fluorescence of the ocular fundus exhibits retinal pigment epithelium lipofuscin characteristics. *Invest Ophthalmol Vis Sci.* 1995;36:718–729.
25. van der Schaft TL, Mooy CM, de Bruijn WC, et al. Early stages of age-related macular degeneration: an immunofluorescence and electron microscopy study. *Br J Ophthalmol.* 1993;77:657–661.
26. Mullins RF, Johnson LV, Anderson DH, et al. Characterization of drusen-associated glycoconjugates. *Ophthalmology.* 1997;104:288–294.
27. Newsome DA, Hewitt AT, Huh W, et al. Detection of specific extracellular matrix molecules in drusen, Bruch's's membrane, and ciliary body. *Am J Ophthalmol.* 1987;104:373–381.
28. Arend O, Weiter JJ, Goger DG, et al. In vivo fundus fluorescence measurements in patients with age related macular degeneration [in German]. *Ophthalmologe.* 1995;92:647–653.
29. Kamei M, Hollyfield JG. TIMP-3 in Bruch's's membrane: changes during aging and in age-related macular degeneration. *Invest Ophthalmol Vis Sci.* 1999;40:2367–2375.
30. Sparrow JR, Parish CA, Hashimoto M, et al. A2E, a lipofuscin fluorophore, in human retinal pigmented epithelial cells in culture. *Invest Ophthalmol Vis Sci.* 1999;40:2988–2995.